A photochemical/thermal switch based on 4,4′-bis(benzimidazolio)stilbene: Synthesis and supramolecular properties

A Photochemical/Thermal Switch Based on 4,4-Bis (benzimidazolio)stilbene: Synthesis and Supramolecular Properties

Shantanu Ganesh Kulkarni,[a] Kristýna Jelínková,[a] Marek Nečas,[b] Zdeňka Prucková,[a] Michal Rouchal,[a] Lenka Dastychová,[a] Petr Kulhánek,*[c] and Robert Vícha*[a]

[a]Dr. S. G. Kulkarni, K. Jelínková, Dr. Z. Prucková, Dr. M. Rouchal, Dr. L. Dastychová, Dr. R. Vícha Department of Chemistry, Faculty of Technology, Tomas Bata University Zlín, Vavrečkova 275, 760 01 Zlín, Czech Republic E-mail: rvicha@utb.cz

[b]Dr. M. Nečas Department of Chemistry, Faculty of Science, Masaryk University, Kamenice 5, 625 00 Brno, Czech Republic

[c]Dr. P. Kulhánek CEITEC - Central European Institute of Technology, Masaryk University, Kamenice 5, 625 00 Brno, Czech Republic E-mail: kulhanek@chemi.muni.cz

Stilbene derivatives are well-recognised substructures of molecular switches based on photochemically and/or thermally induced (E)/(Z) isomerisation. We combined a stilbene motif with two benzimidazolium arms to prepare new sorts of supramolecular building blocks and examined their binding properties towards cucurbit[n]urils (n = 7, 8) and cyclodextrins (β-CD, γ-CD) in water. Based on the ^{1}H NMR data and molecular dynamics simulations, we found that two distinct complexes with different stoichiometry, i.e., guest@β-CD$_1$ and guest@β -CD$_2$, coexist in equilibrium in a water solution of the (Z)-stilbene-based guests. We also demonstrated that the bis(benzimidazo-lio)stilbene guests can be transformed from the (E) into the (Z) form via UV irradiation and back via thermal treatment in DMSO.

Keywords: Stilbene switch, cucurbit[n]uril, cyclodextrins, molecular devices, host-guest systems

1. Introduction

Stilbene moiety appears in many naturally occurring compounds such as well-known resveratrol and synthetic derivatives which have various biological effects.[1] Stilbene, along with its aza- analogues, represents an intriguing structural motif for designing supramolecular components.[2] Illustrative structures that allow for positive charging at both ends of the stilbene moiety, which is important for the binding of cucurbit [n]uril macrocycles (CBns),[3] are shown in **Figure 1**. In addition, these compounds can be used as molecular switches due to their ability to isomerise in response to photochemical and/or thermal stimuli. Such molecular switches can exist in two distinct geometries, represented by (E) and (Z) diastereomers. The (E) isomer shows a straight, rigid arrangement, while the (Z) isomer represents well-defined bent geometry. Due to their different shape, the two isomers can display a contrasting selectivity towards macrocyclic hosts. This phenomenon allowed Harada and colleagues to demonstrate a UV-light-driven adhesion of macroscopic objects.[4] Similarly, Rosales and colleagues were able to reversibly change the mechanical properties of hydrogel fabricated from two sorts of hyaluronan, which were modified with cyclodextrin and azobenzene, respectively.**[5]** Another example of the binding mode switching via a photochemical signal has been described on pillararenes[6] or cucurbit[7]uril,[7] while other studies have demonstrated that the complexation of stilbene inside the cyclodextrin[8] or cucurbit[7]uril cavity,[9] the complementary ditopic 24-crown-8-like host,[10] or within the ternary complex with two molecules of octa acid[11] can significantly influence the ratio of

(E)/(Z) conversion. Stilbene derivatives have also been used as scaffolds for the construction of various supramolecular architectures including crown-ether-based charge-transfer complexes,[12] photochemically controlled hydrogels,[13] and cucurbit[6]uril-based rotaxane.[14] In addition, the (E)/(Z) isomerisation ability of stilbenedisulfonate has been employed in sensing systems, such as in conjugation with oligonucleotides.[15] Further examples can be found in recent reviews.[16]

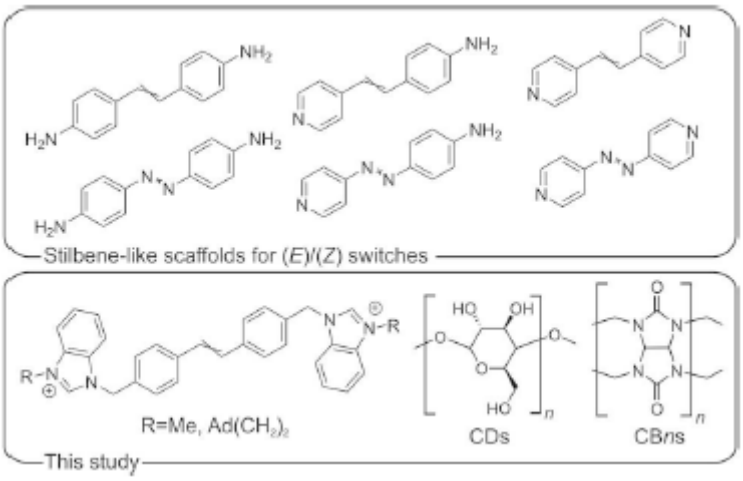

Figure 1. The stilbene-like scaffolds and hosts discussed in this study (n = 7, 8).

Although the studies mentioned above employed diverse macrocycles, there are two families of macrocyclic hosts that have been favoured in most recent supramolecular chemistry. Cyclodextrins (CDs) are natural, biocompatible, and inherently chiral macrocycles that consist of glucose units linked via 1→4 glycosidic bonds to form a conically-shaped structure with nonpolar interior cavity and polar rims decorated with OH groups.[17] The second family, cucurbit[n]urils, are man-made molecular containers with highly symmetric and rigid barrel-like structures. Similarly to CDs, CBns have a non-polar cavity that is capable of binding lipophilic guests via a hydrophobic effect. Moreover, the portals of the CBns cavities are lined with carbonyl groups that can bind cationic species, contributing significantly to overall complex stability. The outstanding binding properties of CBns led to the preparation of the strongest 1:1 complex, with the association constant reaching 10^{17} M^{-1}[18]

Cucurbit[*n*]urils and cyclodextrins can bind guests of similar sizes and shapes[2,19] and can interact with each other via adjacent portals.[20] As a result, they are usually combined with suitable multitopic guests to form functional supramolecular systems such as molecular sensors[21] and catalytic devices.[22]

As a part of our ongoing work on imidazolium-based multitopic guests, we are interested in synthesis, supramolecular behaviour, and the (E)/(Z) isomerisation ability of bisimidazolium salts with stilbene centrepiece, and therefore we prepared two bis(benzimidazolio)stilbene guests to examine the binding ability of their stereoisomers towards β-CD, γ-CD, CB7, and CB8 macrocycles. In this paper, we show that the (Z)-isomer of the guest displays two unexpected distinct binding modes with β-CD, and demonstrate the (E)/(Z) conversion of the guests on UV irradiation and thermal treatment.

2. Results and Discussion

2.1. Synthesis of Guest Compounds

All guests were prepared from the bis(benzimidazolyl) stilbene intermediate **7**. This key intermediate was prepared by a Wittig reaction from the corresponding aldehyde **4** and phosphonium salt **6** (see **Scheme 1**). The preparation of compounds **4** and **6** started from the alcohol **3**, which was oxidized by periodic acid in the presence of Cr^{III} to produce aldehyde **4**. Simultaneously, the alcohol **3** was transformed using SOCp to the corresponding chlorinated compound **5**. Unfortunately, this compound was highly unstable and rapidly underwent polymerization (a non-soluble solid material was formed). As a result, the freshly prepared compound **5** was immediately transformed to the phosphonium salt **6** without any purification. The stilbene **7** arose from the reaction of **4** and **6** as a mixture of (E) and (Z) isomers. The ratio was determined by the integration from the ^{1}H NMR spectrum (FigureS5). Surprisingly, the (Z) isomer predominated in the mixture in the ratio (E):(Z) = 1:2. Although we paid considerable attention to separating these isomers, we did not succeed, and therefore we decided to perform the final quaternization step with the mixture of (E/Z)-**7**.

First, we used MeI to obtain guest **8**, which can be considered as a model for the description ofthe stilbene moiety binding behaviour (Scheme 2). A mixture of (E/Z)-**8** was obtained with the ratio (E):(Z) = 2:3, according to the ^{1}H NMR.

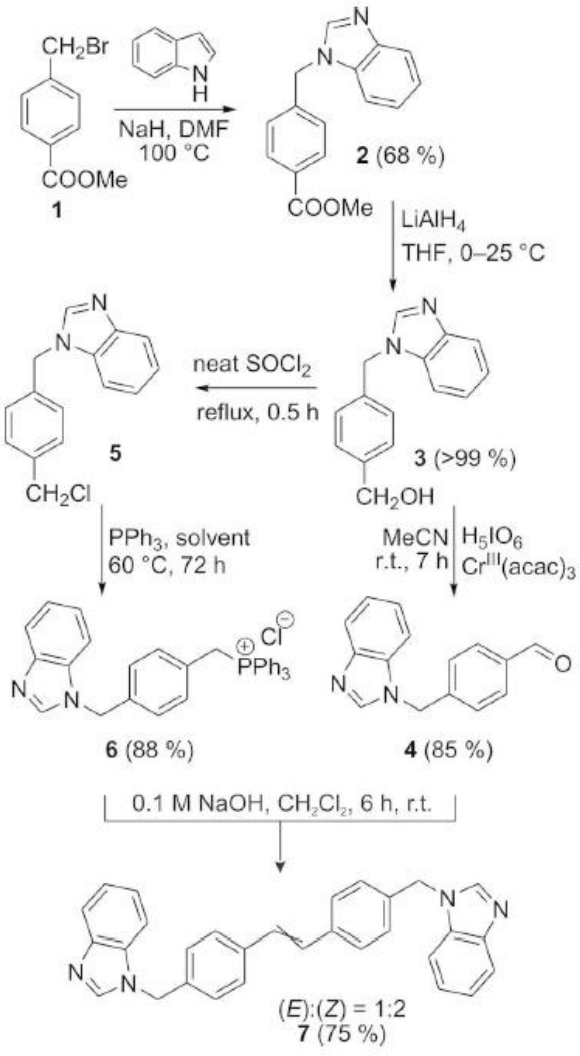

Scheme 1. The synthetic approach towards intermediate **7**.

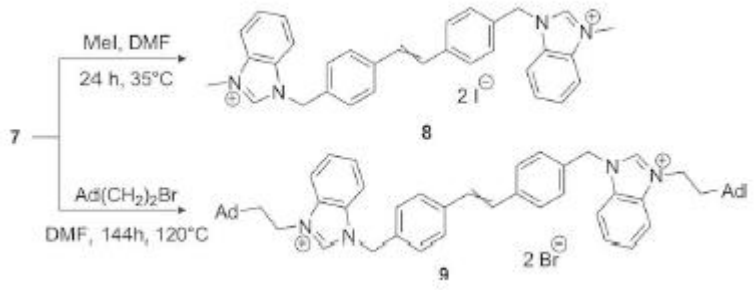

Scheme 2. The procedure towards the stilbene-based guests (Ad = 1-adamantyl).

Fortunately, the solubility of the (E)-isomer markedly differs from that ofthe (Z)-isomer, allowing us to separate essentially pure (E)-**8** by precipitation from the methanol-chloroform mixture. Consequently, the residual mother liqueur contained (Z)-**8**, along with traces of (E)-8, which was removed using column chromatography. It is worth of noting that column chromatography cannot be used directly for the separation of the crude (E/Z)-**8** mixture because we were not able to elute the (E)-**8** isomer.

Finally, we attempted to prepare the hetero-tritopic guest with two terminal high-affinity sites based on 1-adamantyl. Considering the low reactivity of the 1-adamantylmethyl precursors and the effect of the linker between the adamantane cage and the benzimidazolium cation on the affinity towards cucurbit[n]urils, [23] we decided to introduce a 2-(1-adamantyl) ethyl substituent (**Scheme 2**). The reaction mixture was treated for six days at 120°C to reach approximately a 50% conversion of the starting material to the desired (E/Z)-**9** guest, with a (E):(Z) ratio of 1:3 (according to 1H NMR; see, Figure S11). A higher excess of alkylating agent brought no improvement of the yield, while the prolongation of the reaction time and/or a higher reaction temperature led to the conversion of a significant portion of (Z)-**9** to the more thermodynamically stable (E)-**9**. Unfortunately, we were not able to separate these two isomers by a column chromatography or a selective precipitation approach, and so only the (E)-**9** isomer was prepared in a pure form by the extended thermal treatment of the crude mixture of both isomers.

2.2. Assignment of the Structure of the Diastereoisomers

The unambiguous distinguishing of the (E) and (Z) stereoisomers of **8** and **9** was very important for further binding studies. The stilbene motif itself represents one binding site, and its configuration strongly influences the spatial distance between the two other potential binding sites represented by the terminal groups. Since the central double bond in **8** is substituted symmetrically, the distinguishing of the isomers according to the $^{3}J_{HH}$ value in the ^{1}H NMR spectrum is not applicable in this case. Based on previously published NMR data,[9] we can only assume that the isomer with a chemical shift of H—C=C at 6.6 ppm and 7.3 ppm is (Z)-**8** and (E)-**8**, respectively (Figure S6, S8). As will be shown later, the guest **8** forms an inclusion complex with β-CD, which displays a slow exchange mode on the NMR timescale. In such a complex, the two ends of the guest became non-identical, revealing $^{3}J_{HH}$ for the two H-atoms on the central double bond of 12.4 Hz (**Figure 3**). However, such a moderate value of this parameter does not allow for an unambiguous distinguishing of the stereoisomer. Fortunately, we managed to grow a single crystal for the X-ray diffraction analysis via repeated crystallisation from $CHCl_3$ (a slow evaporation of the solvent at room temperature) and determined it as the (Z)-**8**. The ORTEP of the asymmetric unit is shown in **Figure 2** and further details can be seen in Table S1. Note that the (Z)-**8** crystallised with chloride counterions and three water molecules within the asymmetric

unit. We assume that iodide anions were replaced by chloride anions that originated from the oxidative cleavage of $CHCl_3$ during crystallisation. In addition, the single crystal development likely needed some contamination of chloroform solution with moisture.

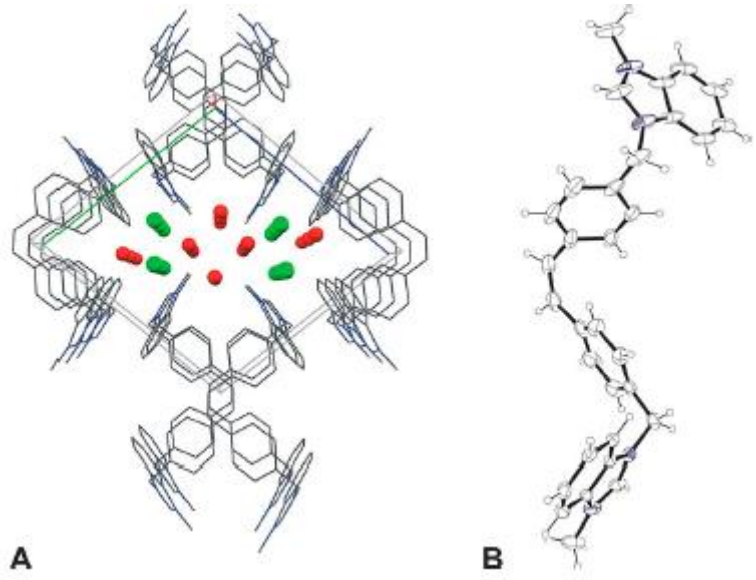

Figure 2. An X-ray diffraction analysis of (Z)-**8**. (A) The crystal packing is viewed down the a-axis. H-atoms are not displayed for clarity. The O-atoms from water and the chloride anions are shown as red and green spheres, respectively. (B) An ORTEP of the asymmetric unit. Water atoms and chloride anions are omitted for clarity.

3. Host-Guest Studies

3.1. NMR Experiments

Initially, we performed several titration experiments with (Z)-**8** in D_2O. Because only one set of signals was observed during titration with CB7 and CB8, we infer that these hosts and (Z)-**8** produced a binding equilibrium that displayed a fast chemical exchange dynamics on the chemical shift timescale (500 MHz, 303 K). In the initial stage of titration with CB7 (up to 1:1 host: guest ratio), the signal of H(j), i.e. **H**—C=C, moved upfield, whereas all other signals moved downfield (Figure S19). This observation could imply the inclusion of the central part of the guest inside the CB7 cavity. However, the H(j)-atoms were shifted downfield and the H-atoms at the benzimidazolium ring, H(g), and H(a) were shifted upfield with an excess of the host. We speculate that upon an excess of CB7, the initial 1 :1 inclusion complex changed to an external 2:1 complex (Z)-**8**@$CB7_2$, with benzimidazolium units sitting at the CB7 portals and terminal methyl groups shallowly buried into CB7 cavities. A similar shifting of the H(j), H(i), and H(h) signals was observed within the titration of (Z)-**8** with CB8 (Figure S20). In contrast to CB7, all the signals of the guest appeared at a lower field, up to the addition of one equivalent of CB8. Upon these observations, we can infer that two binding modes take place at different concentrations of CB8, but that the nature of these complexes cannot be completely clarified using NMR data.

We continued our study on (Z)-**8** with cyclodextrins. Upon the titration of (Z)-**8** with γ-CD, a significant downfield shift of H(a) and H(g-j) signals was observed, as can be seen in FigureS18. Assuming 1:1 binding stoichiometry, the chemical shifts of H(g) and H(j) plotted against the concentration of γ-CD were analysed using the Hanna—Ashbaugh equation[24]as reported previously, [25] to determine the K value to be (6.8± 0.2)x10^3 M^{-1}. The most interesting results were obtained using β-CD as a host (**Figure**

3, Figure S17). We observed two separate set of signals for the guest. One of the sets displayed broadened proton signals that shifted downfield upon incremental addition of the host (see the signals marked by asterisks in **Figure 3**). This observation indicates the formation of a complex in the mixture displaying a moderate-exchange mode. The second set of signals did not experience chemical shift changes but featured an increase in intensity at the expense of that of the former. In the presence of two equivalents of the host, only the second set of signals was detected. This indicated the formation of another complex in a slow-exchange mode.

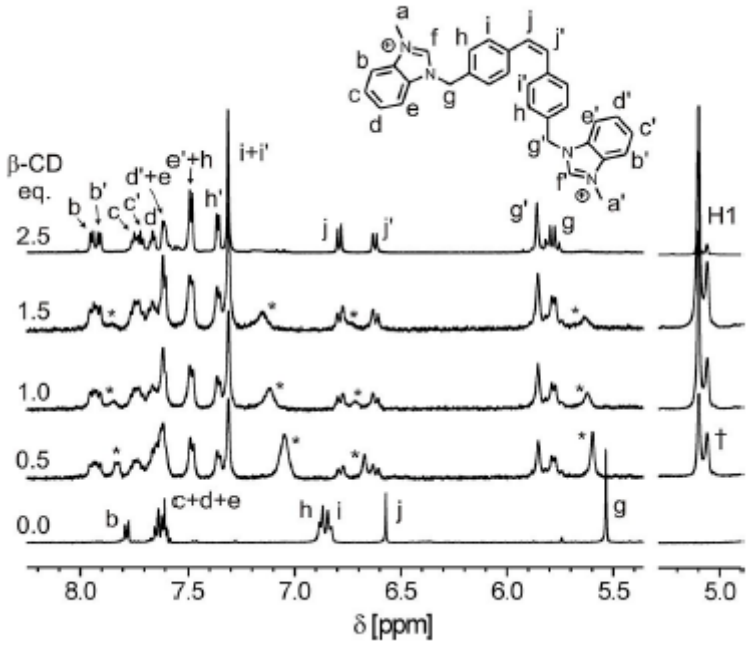

Figure 3. A portion of the ^{1}H NMR spectrum of the (Z)-**8**/β-CD mixture in D_2O, recorded at 500 MHz (700 MHz for the upper line). The signals assigned to the guest that bound in the moderate-exchange manner are asterisked. The H^1 signal (this part of the spectra was downscaled three times) for β-CD which is bound in the slow-exchange mode is marked with t.

Note that the signals of the second set are split into pairs likely due to the inherently chiral β-CD. [25] Two observations should be stressed. First, the complete conversion from the moderate-to the slow-exchanged complex requires two equivalents of β-CD. Second, the examination of the integral intensities of H(g) and H^1 after the deconvolution revealed that the ratio was 1 :1 at each step of the titration. This suggests that the slow-exchange complex consists of two β-CD units, but only one macrocycle is bound in the slow-exchange manner. To shed light on this intricate complexation behaviour, we performed a number of molecular dynamics simulations (see **Section 3.4** below). The supposed structures of the (Z)-**8**@β-CD and (Z)-**8**@p-CD_2 complexes are shown in **Figure 4**.

The low solubility of (E)-8 in a water environment discourages any quantitative analysis of NMR data, and therefore only qualitative information will be summarised further. In titration experiments with β-CD, we observed very similar ^{1}H NMR signals pattern for (E)-**8** as for (Z)-**8**. As can be seen in Figure S21, the signals of H-atoms at terminal methyl groups H (a), methylene bridges H(g), and central double bond H(j) were split into pairs likely due to the complexation of the guest inside the conical CD cavity in a slow-exchange manner. In titration experiments with CB7, we observed an unambiguous upfield shift of the signal of the H-atom at the central double bond. This observation indicates the formation of an inclusion complex with a stilbene centrepiece, positioned inside the CB7 cavity. We also

performed some experiments in mixed solvents, namely in the mixture D_2O:DMSO-d_6 (1:1, v:v), but only very small shifts of signals indicated the formation of very weak complexes, if any (Figure S23).

Finally, we examined the guest (E)-**9**, which was insoluble in pure water, according to the ^{1}H NMR spectrum. However, the addition of a large excess of β-CD (approximately 5 eq.) led to the partial dissolving of the guest due to the formation of a water-soluble complex (Figure S25). Knowing that adamantane derivatives usually form highly stable inclusion complexes with β-CD (log K = 4-5), it is reasonable to suppose the positioning of CD at the terminal (T) adamantane sites. In addition, the splitting of signals from the central part of the guest indicates that the central (C) stilbene site is also occupied by cyclodextrin likely to form a 1:3 assembly (E)-**9**@(β-CD^C, β-CD$_2^T$), where C and T superscripts denote the central and terminal sites of the guest, respectively.

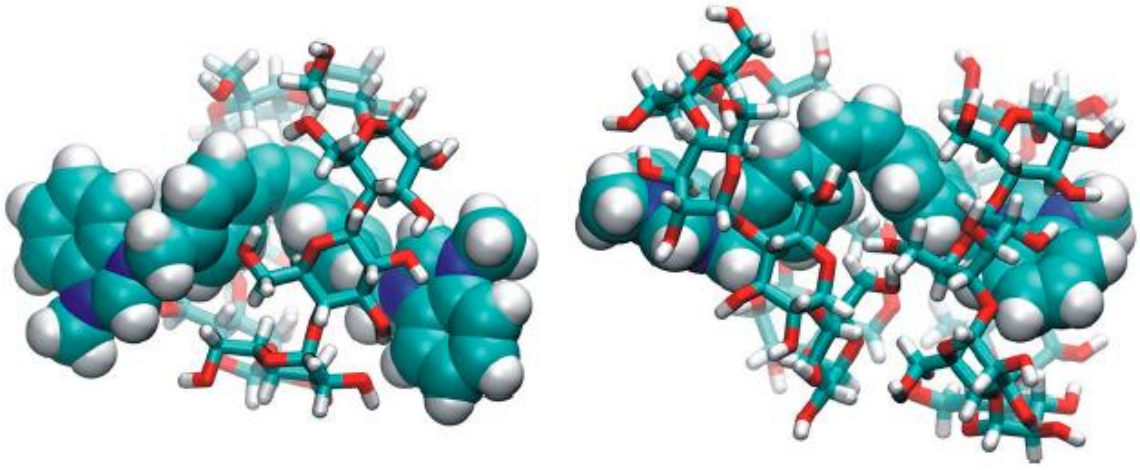

Figure 4. Representative structures of the (Z)-**8**@p-CD (left) and (Z)-**8**@β-CD_2 (right) as obtained from MD simulations.

Note that in the less polar medium (CD_3OD: D_2O, 2:1, v:v), only the occupation of the terminal adamantane sites was observed (Figure S27). Contrary to β-CD, the addition of the CB7 to the dispersion of the guest (E)-**9** in water did not improve solubility, and only the signals of CB7 were observed in the ^{1}H NMR spectrum. However, the addition of CB7 into the solution in which the quaternary aggregate (E)-**9**@(β-CDC, β-CD$_2^T$) predominates (see above) led to the rapid upfield shift of the adamantane signals as the β-CD units at terminal sites were replaced with CB7 macrocycles. Nevertheless, the remainder of the complex in the solution indicates that (E)-9@(β-CD^C, CB7$_2^T$) was formed, most likely because the formation of (E)-**9**@(CB7$_2^T$) with an excess of CB7 was not observed as described above. This hypothesis is supported by the observation of two distinct sets of signals for β-CD. The minor signal can be attributed to the β-CD, which is fastened at the central stilbene site by two CB7 stoppers, as described previously with different guests. [26]

3.2. Titration Calorimetry

As mentioned above, the guests (E)-**8** and (E)-**9** displayed very low solubility in a water environment, and therefore we were not able to conduct any reasonable ITC experiment with (E)-**9**, and titrations with (E)-**8** were limited to the more stable complexes with CBns.

The experimental values of the association constants K of (Z)-**8** with β-CD and γ-CD are very similar (see **Table 1**). If we consider the binding of the central part of the guest inside the cyclodextrin cavity,

the stronger binding of the bulky (Z)-**8** with the wider γ-CD could be expected. The comparable K values, which were obtained using a One Set of Sites model, imply that binding modes are different. We assume a conventional inclusion binding mode with the central part of the (Z)-**8** guest inside the γ-CD cavity. On the other hand, the situation is intricate in the (Z)-**8** + β-CD system. We employed three theoretical models available in Origin software, i.e., One Set of Sites (OSS), Two Sets of Sites (TSS), and Sequential Binding Sites (SBS), to analyse these data (Figure S56). Whereas the TSS model did not provide any meaningful results, similar K values were obtained using OSS and SBS model. Assuming 1:2 stoichiometry of the complex, the OSS model provided average K value, while K^1 and K^2 values, which were calculated using the SBS model, indicate a positive cooperativity of the β-CD units. **[27]**

Table 1. The K [M^{-1}] values obtained by the ITC in water at 303 K.

	(*Z*)-8	(*E*)-8
β-CD[a]	$(2.44 \pm 0.18) \times 10^3$	NA
β-CD[b]	$K_1 = (3.1 \pm 0.2) \times 10^3$	NA
	$K_2 = (1.55 \pm 0.03) \times 10^3$	NA
γ-CD[c]	$(6.8 \pm 0.2) \times 10^3$	NA
CB7[a]	$(1.94 \pm 0.05) \times 10^5$	$(5.5 \pm 1.3) \times 10^6$
CB8[a]	$(5.1 \pm 0.7) \times 10^7$	$(4 \pm 2) \times 10^8$

[a]One Set of Sites model; [b]Sequential Binding Sites model (2 sites); determined by ^{1}H NMR titration in D_2O at 303 K; NA = not available due to the low solubility of the guest.

As suggested by the ^{1}H NMR results and computational data (see below), the binding sites for β-CD units within 1: 1 and 1:2 complex are different. Transformation of the 1:1 complex to the 1: 2 complex involves dissociation of the β-CD unit from the centre of the guest and binding of the two β-CD units at terminal binding sites. Therefore, ITC data for the (Z)-**8** + β-CD system are only indicative and the experimental values of K provided in **Table 1** for must be considered to be apparent. The complexes of both guests **8** with CB7 and CB8 display moderate stabilities, as can be seen in **Table 1** (the complete thermodynamic data are in Table S2, while the binding isotherms are shown in Figure S55 and Figure S57, respectively). The weakest complex was observed for (Z)-8 with CB7. This relatively low stability can likely be attributed to the steric strain of the bent guest molecule inside the narrow CB7 cavity. In contrast to the (Z)-**8**, the straight guest (E)-**8** is better suited to the CB7 cavity, with 28 x higher K value in comparison to the (Z)-**8**@CB7 complex. It is a somewhat surprising that (E)-**8** binds the CB8 significantly stronger than CB7. The corresponding K_{CB8}/K_{CB7} ratio is 72.7. Since the distance between the two N-atoms adjacent to the central stilbene part in the guest (E)-**8** is about 14 Å and the portal-portal distance in CBn is about 9 Å, it is reasonable to suppose that CB7 runs between the two termini, while only one portal is effectively involved in the ion-dipole interaction. In contrast, the higher stability of the (E)-**8**@CB8 complex can be explained by the tilting of the guest inside the wider cavity to allow the contribution of both CB8 portals to the complex stabilisation.

3.3. Mass Spectrometry

Finally, we employed an ion-trap mass spectrometer with an electrospray ion source to provide independent support for the assumed complexes. We analysed the equimolar mixtures of the guests (Z)-8, (E)-**8**, and (E)-**9** with β-CD, γ-CD, CB7, and CB8 in concentrations of 6.3 μM. In all the studied

cases, we observed signals related to the doubly charged [guest-host]$^{2+}$ complexes. In the mixtures of both isomers of guest **8** with two equivalents of the largest macrocycles, i.e., γ-CD and CB8, we observed weak but unambiguous signals of the [guest-host$_2$]$^{2+}$ aggregates. To support a 2:1 binding stoichiometry in the case of (Z)-**8** and β-CD, we measured the spectrum of the solution with a large excess of β-CD (5 equivalents). We observed weak but unambiguous signals of (Z)-**8**@β-CD$_2$, as can be seen in Figure S31B. In the case of the guest (E)-**9**, the aggregates of the [guest-host$_2$]$^{2+}$ type were observed with both CB7 and CB8, respectively. Finally, we studied the ability of (E)-**9** to form quaternary complexes in the gas phase. In all of studied mixtures containing three equivalents of β-CD or γ-CD and five equivalents of CB7 or CB8, a triply charged signal assigned as the [guest-CD,CB$_2$ + Na$^+$]$^{3+}$ was observed. For the corresponding spectra, see Figures S30-S54 in the Supporting Information.

3.4. (Z)/(E) Isomerisation

We performed several experiments to examine the ability of prepared guests to switch their geometry via the isomerisation of the central stilbene double bond. All these experiments were carried out in borosilicate glass NMR tubes, and the composition of the reaction mixtures was determined using ^{1}H NMR spectroscopy. As mentioned in Section 2.1., the compound (Z)-**9** can be readily transformed into its (E isomer by thermal treatment. In contrast, the pure (Z)-**9** was not available due to difficulties within purification, and therefore we started with pure (E)-**9** (the ^{1}H NMR spectrum in d$_6$-DMSO is shown in **Figure 5**, line 1), which was immersed into an acetone bath and irradiated using a medium-pressure mercury lamp (125 W). The acetone filter was used to avoid an undesired 2π + 2π cycloaddition. In 90 minutes, a photostationary state (E)-**9**:(Z)-**9** = 52:48 was reached (for the ^{1}H NMR spectrum, see Figure 5, line 2). Similarly, pure (E)-8 produced a mixture of (E)-8:(Z)-8 = 42:58. Subsequently, we treated these mixtures in DMSO at 120±2°C to obtain complete recovery of (E)-**9** within 16 hours (for the ^{1}H NMR spectrum, see **Figure 5**, line 3). We repeated the photochemical/thermal cycle five-times with compound 9 to observe essentially the same (E):(Z) ratios in each step, as the inserted chart demonstrates in **Figure 5**. Only insignificant amount of side products was detected via ^{1}H NMR spectra. Surprisingly, the compound (Z)-**8** underwent thermal isomerisation very slowly under the same conditions to produce only 5% of (E)-**8** within 10 hours. In addition, we repeated all the above-mentioned experiments in the presence of β-CD and CB7, respectively, but observed no significant influence of the hosts on the (E):(Z) ratio. To conclude this section, we infer that structures derived from stilbene **9** are suitable candidates for the construction of photochemical-thermal molecular switches.

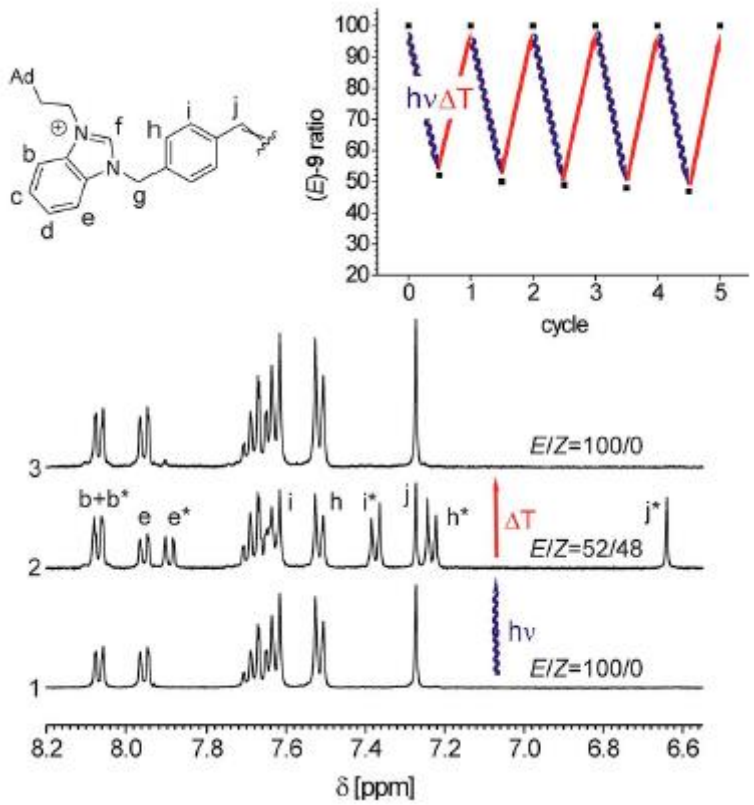

Figure 5. A portion of the ^{1}H NMR spectra of the (E/Z)-**9** mixture in d6-DMSO, recorded at 400 MHz. The signals assigned to the (Z)-**9** are asterisked. Line 1 starts (E)-**9**; the line 2 mixture after 90 minutes of irradiation; and the line 3 mixture after 16 hours of treatment at 120 °C. The inserted chart demonstrates reproducibility within five cycles.

3.5. The Computed Binding Modes of (Z)-8, (E)-8 and β-CD

As mentioned above, we faced certain difficulties interpreting the binding behaviour of (Z)-**8** towards β-CD from NMR and ITC data, which suggests that there are at least two distinct binding modes. To shed light on this issue, we performed extensive molecular dynamic simulations on the 1: 1 (Z)-**8**@β-CD complex.

Initially, we performed an unbiased MD simulation to reveal that the complex is stable during the 1-μs-long simulation (Figure S61). Most of the time, the stilbene part of the guest was inside the cavity of cyclodextrin ($0.35 < \tau < 0.75$; τ is a collective variable that describe the transition of the guest through the β-CD cavity, see below and the Supporting Information section for more detail). We also observed transitions to the other state ($0.85 < \tau < 0.95$), in which one of the benzimidazolium terminals was moved to the cavity, while the rest of the guests pointed to the space of the primary CD rim. The other possibility, in which the guest would point to the space of the secondary CD rim, was not observed. A possible cause of this observation would be the separation of such a state by a barrier, which discourages visiting such a state on a time scale accessible by unbiased MD simulation (< 1 μs).

To test this hypothesis, we employed the biased MD simulation to obtain detailed information about a possible shuttle of β-CD alongside the guest.

In general, biased MD simulations require the correct selection of suitable geometrical parameters, also called collective variables (CV), along which the bias is employed. The bias helps to promote transitions that would be otherwise unobserved in regular MD simulations in a computationally accessible time scale. In our work, we tried to understand the shuttling of β-CD alongside guest, or in other words, the threading of the (Z)-**8** guest through the cavity of the cyclodextrin host. We found that these movements are complex because both host and guest are very flexible. In the case ofthe guest, the flexibility is introduced by methylene linkers (carbon atoms C11 and C26, Figure S58) between otherwise rigid blocks composed of the central stilbene and terminal benzimidazolium parts.

We tested several standard collective variables such as distances and angles and their combinations, but their performance was found to be unsatisfactory, and therefore we implemented new collective variables that were designed to handle the threading of a flexible guest through the cavity of the host (Figure S60). The collective variable t describes the parametric position of the guest in the cavity, taken from the intersection between the plane representing the host and the guest worm-like representation. We found that this CV alone was not able to facilitate back-and-forth transitions due to a significant hysteresis along the pathway, and therefore we had to include another collective variable χ, which facilitated smoother movement. This CV describes the direction of the guest portion within the cavity. The result of the biased simulation employing these two CVs is shown in Figure S62A.

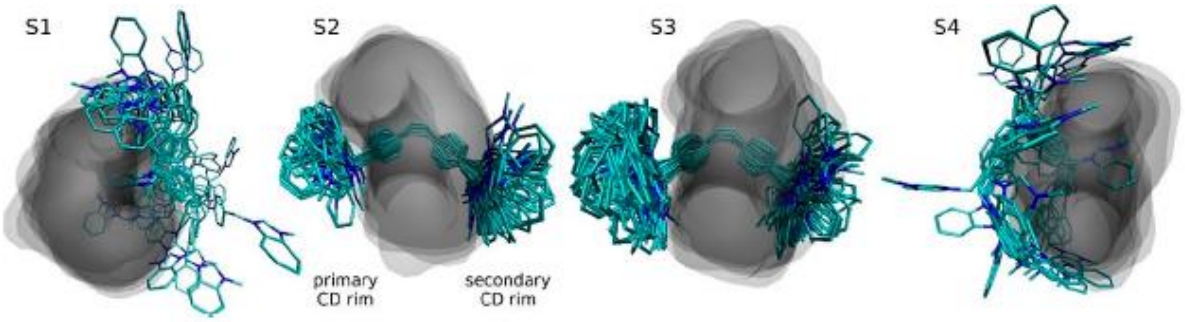

Figure 6. Representations of the detected thermodynamic states **S1** to **S4** of the (Z)-**8**@β-CD complex. The guest is shown using the stick model, while the host is displayed using the semi-transparent molecular surface. The cavity is indicated by the darkest region. Hydrogen atoms are not shown for clarity. To further improve the visualisation deception, the guest was superimposed using the benzimidazolium ring for the **S1** and **S4** states, and the stilbene part for the **S2** and **S3** states.

Altogether, we found four states **S1-S4**. States **S2**, **S3**, and **S4** were already observed in unbiased MD simulation, while the state **S1** was new. Unfortunately, we were not able to capture it entirely because a complex dissociation occurred for τ < -0.02. The geometrical representation of the found states is shown in **Figure 6**. Since the x collective variable played a supplementary role, we removed it by statistical reweighing. The obtained free energy profile $\Delta G_w(\tau)$ describing the threading is shown in **Figure 7**, and the energies of the found states and transition states are summarised in Table S6.

In the **S2** and **S3** states, the stilbene part of the guest is placed inside the cavity of the host. The main difference lies in the position of the guest towards the CD rims. In **S2**, the primary CD rim is closer to one of the benzimidazolium terminals, while in **S3**, it is the secondary CD rim. The obtained free energies showed that the **S3** arrangement is somewhat beneficial, in comparison to **S2**. However, the

energy difference (0.5kJmol^{-1}) and the barrier separating these states (~ 1.4kJmol^{-1}) is very small, suggesting that they are effectively one state.

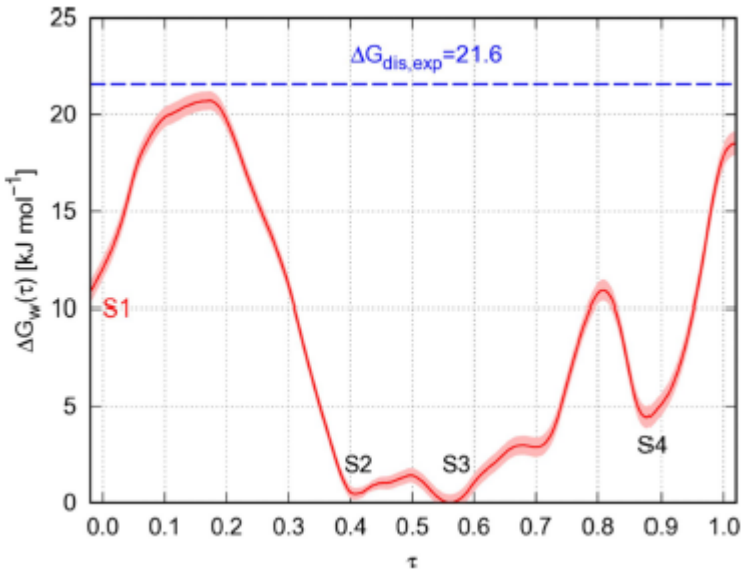

Figure 7. The free energy profile ΔG_w (τ) for the guest (Z)-**8** threading through the cavity of the β-CD obtained from the 5.0-μs-long ABF/MWA simulation. The identified thermodynamic states are labelled **S1** to **S4**. The confidence intervals (errors) of the calculated free energy are shown as a light colour strip. The experimental dissociation energy from the ITC experiment is indicated by a blue dashed line.

In the **S1** and **S4** states, the cavity is occupied by one of the benzimidazolium terminals, instead of the stilbene part. In most cases, the guest has a 'C'-like shape in which the other benzimidazolium terminal interacts with the outer surface of the host (Figure S63). Interestingly, the orientation of the benzimidazolium terminals in the cavity differs. In S1, the benzene ring is buried in the cavity, while the imidazole ring is located at the entrance of the secondary CD rim. In **S4**, the benzimidazolium ring is deeply immersed into the cavity and rotated by about 90°.

We also attempted to create a model of a possible 1:2 complex (Z)-**8**@β-CD_2. Due to the limited experimental evidence about the potential arrangement, we considered all three orientations of the β-CD rims. Only one arrangement was stable during the entire 1-μs-long unbiased MD simulation (Table S4). In this arrangement, β-CDs were faced by their primary CD rims (P…P). The other arrangements were unstable and led to the complex dissociation; i.e. one of p-CDs slipped from the guest to form the 1:1 complex. This was proved by multiple repeats of the simulations that were started from different initial configurations.

The structure of the stable 1:2 arrangement is shown in Figure S64. Although both the guest and the P…P arrangements of the β-CDs are symmetrical, a detailed analysis of the β-CD positions over the guest revealed the temporal asymmetry of two p-CDs towards the guest (Figure S65). This observation is drawn from the relatively short simulation (1μs) performed on a time scale that is far away from the slow-exchange NMR timescales. However, the arrangement complexity, where multiple hydrogen bonds exist at the interface of two rims, suggests there might be a sufficiently large barrier, making this temporal asymmetry experimentally observable.

Subsequently, we focused on the guest (E}-**8**. The complex (E)-**8**@β-CD was stable during the entire 1-μs-long unbiased MD simulation. β-CD was positioned over the stilbene part of the guest with no transitions to the benzimidazolium terminals, as observed in the case of (Z)-**8**@β-CD. The representative structure and progress of t are shown in Figure S66 and Figure S67, respectively.

Similarly to the complexes containing (Z)-8, only one arrangement of two p-CDs (P…P) was stable during the entire simulation of (E)-**8**@p-CD_2 (Table S4). The representative structure and progress of τ are shown in Figure S68 and Figure S69, respectively.

An analysis of the radial distribution functions between the water oxygen atoms and hydrogen atoms on the C18 and C19 carbons of the guest showed markedly lower values for complexes containing the guest in the (E)-configuration than their (Z)-counter parts, with only minor impact by complex stoichiometry (Figure S70). This indicates that the stilbene core is more efficiently wrapped by β-CD(s) when the guest has a straight-like shape due to the (E)configuration, rather than a bent-like shape due to the (Z)-configuration.

4. Conclusion

We prepared three guests based on a new bisbenzimidazolium binding motif with a stilbene centrepiece, and described their binding properties towards cucurbit[n]urils and cyclodextrins. Using titration calorimetry, we determined the association constants of guest **8** with β/γ-cyclodextrins and CB7/8 in an order of magnitude of $10^3 M^{-1}$ and 10^{5-8} M^{-1} respectively. Interestingly, the ^{1}H NMR titrations revealed that the supramolecular system consisting of β-CD and guest (Z)-**8** displays distinct binding modes, with a different exchange rate on the NMR timescale. However, an extensive biased MD simulation of the (Z)-**8**@β-CD complex revealed that p-CD can move along the guest despite its curved shape, with only small barriers. In the most stable configurations (**S2** and **S3**, $\sim$ 0 $kJmol^{-1}$), β-CD is positioned over the stilbene core, while in the less stable configurations (**S1** and **S4**, 10.9 and 4.4 $kJmol^{-1}$), β-CD is positioned over either terminal benzimidazolium ring. These two states are slightly different due to the inherent asymmetry of β-CD. The natural asymmetry of the complex due to β-CD could be responsible for the observed asymmetry of the ^{1}H NMR signals of the guest, upon interaction with β-CD. On the other hand, the calculated barriers and comparison with the experimental binding affinity (—21.6$kJmol^{-1}$) indicate that such a complex can exist in the fast-exchange regime of NMR.

Considering this and the fact that the complex in a fast-exchange manner was observed within the ^{1}H NMR titration up to two molar excess of β-CD, we infer that the splitting of the ^{1}H signal observed during the NMR titration of (Z)-**8** with β-CD can be attributed to a (Z)-**8**@β-CD_2 that coexists in the mixture along with (Z)-**8**@β-CD from the early stage of the titration experiment.

Unbiased MD simulations on the (Z)-**8**@β-CD_2 complex revealed that only an arrangement with CDs facing each other with the primary rims is stable. Although this geometry is symmetrical, an analysis of 1-μs-long MD simulation revealed a temporal asymmetry of the complex, and therefore the observed slow-exchange NMR signals can be explained by higher kinetic barriers between the states showing temporal asymmetry. Even though this is not fully supported by our simulations because of the significantly shorter simulation times (ps) in comparison to the expected time scales in the slow-exchange NMR regime (ms), it is supported by the structure itself. There is a significant amount of hydrogen bonds at the CD interface that need to be rearranged. Their reorganisation can be slow enough to provide slow-exchange NMR signals.

For comparison, we also modelled 1:1 and 1:2 complexes containing (E)-**8**. Qualitatively, these complexes behave similarly to those containing (Z)-**8**. One noticeable difference lies in the way the central part of the stilbene is covered by β-CD. Due to the bent structure of the (Z)-**8** guest, the hydrogen atoms at the C18 and C19 carbons are more exposed to the solvent than in the case of (E)-**8**.

Finally, we demonstrated that the reversible conversion of the (Z) → (E) and (E) — (Z) configurations of the guests can be achieved by thermal and photochemical treatment, respectively. Since the stereoisomers differ in their binding properties, the bis(benzimidazolio) stilbene motif is a suitable candidate for the construction of molecular switches.

Experimental Section

General

All solvents, reagents, and starting compounds (if not mentioned otherwise) were of analytical grade, purchased from commercial sources and used without further purification. 1-(1-Adamantyl)-2-bromoethane was prepared as described previously.[23] The photochemical experiments were conducted in commercial photochemical borosilicate glass reactor (Photochemical Reactors Ltd, UK) using a medium pressure mercury lamp (125 W). **Melting points** were measured on a Kofler block and are uncorrected. Elemental analyses (C, H and N) were determined with a Thermo Fisher Scientific Flash EA 1112. **NMR spectra** were recorded at 303 K on a Bruker Avance III 500 spectrometer operating at frequencies of 500.11 MHz (1H) and 125.77 MHz (13C), on a Jeol JNM-ECZ400R/S3 spectrometer operating at frequencies of 399.78 MHz (^{1}H) and 100.53 MHz (^{13}C), and on a Bruker Avance III 300 spectrometer operating at frequencies of 300.13 MHz (1H) and 75.77 MHz (^{13}C). The ^{1}H- and ^{13}C-NMR chemical shifts were referenced to the signal of the solvent [^{1}H: S(residual $CHCl_3$) = 7.26 ppm, δ(residual HDO) = 4.70 ppm, δ(residual DMSO-d_5) = 2.50 ppm; ^{13}C: S(DMSO-d_6) = 39.52 ppm, δ($CDCl_3$) = 77.16 ppm]. Signal multiplicity is indicated by 's' for singlet, 'd' for doublet, 'dd' for doublet of doublets, 'm' for multiplet, and 'um' for an unresolved multiplet. **IR spectra** were recorded using a Smart OMNI-Transmission Nicolet iS10 spectrophotometer. Samples were measured in KBr discs. **UV-Vis spectra** were recorded using a Thermo Spectronic spectrophotometer within a range of λ = 280-800 nm, with a 2 nm step. **Electrospray mass spectra** (ESI-MS) were recorded using an amaZon X ion-trap mass spectrometer (Bruker Daltonics, Bremen, Germany) equipped with an electrospray ionization source. All the experiments were conducted in the positive-ion polarity mode. The instrumental conditions used to measure the single imidazolium salts, and their mixtures with the host molecules were different, so they are described separately. Single imidazolium salts: Individual samples (with concentrations of 0.5 μg cm^{-3}) were infused into the ESI source in methanol:water (1:1, v:v) solutions using a syringe pump with a constant flow rate of 3 μl min^{-1} The other instrumental conditions were as follows: an electrospray voltage of -4.2 kV, a capillary exit voltage of 140 V, a drying gas temperature of 220°C, a drying gas flow rate of 6.0 dm^3min^{-1}, and a nebulizer pressure of 55.16 kPa. Host-guest complexes: An aqueous solution of the guest (6.25 μM) and the equimolar amount of the corresponding host (in the case of γ-CD and CB8, respectively, experiments with 2.0 eq. of these hosts were also carried out) for the binary complexes or an aqueous solution of the guest molecule (6.25 μM), CB7/8 (3.0 eq.), and β/γ-CD (5.0 eq.) for the ternary complexes, was infused into the ESI source at a constant flow rate of 3 μl min^{-1}. The other instrumental conditions were as follows: an electrospray voltage of -4.0 kV, a capillary exit voltage of 140 V up to -50 V, a drying gas temperature of 300°C, a drying gas flow rate of 6.0 dm^3min^{-1}, and a nebulizer pressure of 206.84 kPa. Nitrogen was used as both the nebulizing and drying gas for all of the experiments. Tandem mass spectra were

collected using CID with He as the collision gas after the isolation of the required ions. **Isothermal titration calorimetry** measurements were carried out in H_2O using a VP-ITC MicroCal instrument at 303 K. The concentrations were approximately 0.130.15 and 0.46-0.50 mM for the host in the cell and the guest in the microsyringe, respectively. The raw experimental data were analysed with the MicroCal ORIGIN software. The dilution heats were taken into account for each guest compound. The data were fitted to a theoretical titration curve using the 'One Set of Binding Sites' model. A methylviogen dichloride hydrate with association constant of 7.05 10^6 dm^3mo^{-1} was used as competitor. **Diffraction data** were collected on a Rigaku MicroMax-007 HF rotating anode four-circle diffractometer using Mo Kα radiation at 120 K. Crystal-Clear and CrysAlisPro software packages were used for data collection and reduction. [28] The structures were solved by the direct methods procedure and refined by full matrix least-squares methods on F^2 using SHELXT and SHELXL.[29] All non-hydrogen atoms were refined anisotropically. Water hydrogens were not easily located in the difference Fourier maps, and therefore not included in the refinement. All other hydrogen atoms were refined as riding on their carrier atoms. The supplementary crystallographic data for this paper can be obtained free of charge from the Cambridge Crystallographic Data Centre (reference no. 1908033) via www.ccdc.cam.ac.uk/data_request/cif.

Computational Methods

Molecular dynamics simulations of the (Z)-**8**@β-CD, (Z)-8@p-CD_2, (E)-8@β-CD, and (E)-**8**@β-CD_2 complexes were performed in the Amber 16 package[30,31] and a modified pmemd program from AMBER connected with PMFLib. [32] The β-CD host and (Z/E)-**8** guests were described by the GLYCAM[33] and GAFF[34] force fields, respectively. Each complex was immersed into a truncated octahedral box filled by the TIP3P water[35] and two chloride anions[36] to maintain electroneutrality. The temperature and pressure were kept at 300 K and 100 kPa, respectively. The concentration of the complex under the employed conditions was between 10 and 19 mM. In addition to the unbiased MD simulations, which were each 1 μs in length, we run 5-μs-long biased simulation of the (Z)-**8**@β-CD complex in the space of two collective variables, t and x, employing the Adaptive Biasing Force (ABF) method[37-38] enhanced by the Multiple-Walker Approach (MWA). [39-40] The collective variable τ aimed to determine the parametric position of the guest towards the host, while the supplementary collective variable χ determined the directionality of the guest within the cavity. The free energy landscape was obtained by the integration of the calculated mean forces from the ABF/MWA simulation using Gaussian Process Regression (GPR).[41-42] Since the χ collective variable played a supplementary role, we removed it by statistical reweighting, which provided the free- energy profile of the threading $\Delta G_w(\tau)$. Errors were estimated using GPR and are reported in the form of the confidence interval provided at three standard deviations. A detailed description of the computational methods is given in the Supporting Information.

Synthesis

Methyl 4-((1H-benzo[d]imidazol-1-yl)methyl)benzoate (2)

Benzimidazole (7.11 g, 60.24 mmol) was dissolved in DMF (100 cm^3) under a nitrogen atmosphere. NaH (60% suspension in mineral oil, 2.91 g, 72.79 mmol) was added portionwise over a period of 10 min. The reaction mixture was stirred at room temperature for 30 min and ester **1** (11.50 g, 50.2 mmol) was added. The colourless mixture became dark red and was heated to 100°C for 4 h. The reaction progress was monitored by TLC and/or GC-MS. Upon completion, the reaction mixture was cooled to

room temperature and poured over crushed ice to quench an excess of NaH. The crude product was extracted with EtOAc, and the collected organic portions were washed with ice-cold H_2O to remove DMF and dried over anhydrous Na_2SO_4. Subsequently, the solvent was removed under a vacuum and the crude material was purified in silica gel column eluted with MeOH:$CHCl_3$ (2:98, v:v) to obtain pale yellow 2 (9.06 g, 68% yield with respect to **1**). M.p.: 101-103 °C (lit.[10] 102-103 °C). The obtained ^{1}H NMR spectrum matches the data reported previously. [43]

(4-((1H-benzo[d]imidazol-1-yl)methyl)phenyl)methanol (3)

A solution of methyl ester 2 (2.50 g, 9.39 mmol) in 15 cm^3 of dry THF was added dropwise to the suspension of LiAlH4 (1.78 g, 46.89 mmol) in THF (30 cm^3) at 0°C over a period of 15 min. The reaction was warmed up to room temperature and stirred for 3 h under a nitrogen atmosphere, and the reaction progress was monitored by GC-MS. Upon completion, the reaction mixture was quenched by AcOEt (8 cm^3). The colourless solid, which appeared within a few minutes of stirring at 0°C, was filtered off and washed with plenty of AcOEt. Collected organic portions were washed with H_2O (50 cm^3) and dried over anhydrous Na_2SO_4. The solvent was removed under a vacuum to obtain the crude product. Pure alcohol **3** was obtained by column chromatography (silica gel, MeOH:$CHCl_3$ (2:98, v:v) as a pale yellow solid (2.23 g, > 99%). M.p.: 137-139°C. Anal. Calcd. for $C_{15}H_{14}N_2O$ (238.28) C 75.61, H 5.92, N 11.76. Found C 75.43, H 6.07, N 11.85. ^{1}H NMR (400 MHz, DMSO-d_6): δ 4.46 (s, 2H), 5.14 (um, 1H), 5.48 (s, 2H), 7.20 (um, 2H), 7.28 (um, 4H), 7.51 (um, 1H), 7.67 (um, 1H), 8.43 (s, 1H) ppm. $^{13}C\{^1H\}$ NMR (100 MHz, DMSO-d_6): δ 47.5, 62.5, 110.7, 119.4, 121.6, 122.4, 126.7, 127.2, 133.6, 135.1, 142.1, 143.3, 144.2 ppm. IR (KBr disc): 424 (w), 505 (w), 569 (w), 719 (w), 740 (s), 779(m), 829 (w), 893 (w), 958(w), 979 (w), 1016 (m), 1173 (w), 1190 (m), 1261 (m), 1284 (m), 1346 (w), 1381 (w), 1421(w), 1458 (m), 1496 (s), 1614 (w), 2341 (w), 2360 (m), 2862 (w), 2935 (w), 3259 (bs) cm^{-1}.

4-((1H-benzo[d]imidazol-1-yl)methyl)benzaldehyde (4)

H_5IO_6 (3.47 g, 15.22 mmol) was dissolved in dry MeCN (30 cm^3) under a nitrogen atmosphere and subsequently, $Cr^{III}(acac)_3$ (0.27 g, 7.61 mmol) and **3** (1.81 g, 7.60 mmol) were added. The reaction mixture was stirred at room temperature for 7 h, and the reaction progress was monitored by GC-MS and/or TLC. After completion, a saturated solution of Na_2SO_3 (100 cm^3) was added and the mixture was extracted with AcOEt (3x400 cm^3). The collected organic portions were dried over anhydrous Na_2SO_4 and the solvent was removed under a vacuum. The crude material was purified on a column (silica gel, MeOH:$CHCl_3$ (2:98, v:v)) to obtain an off-white solid **4** (1.52 g, 85%). M.p.: 125-127 °C. ^{1}H NMR (500 MHz, $CDCl_3$): δ 5.56 (s, 2H), 7.26-7.38 (m, 5H), 7.85-7.89 (m, 3H), 8.55 (s, 1H), 9.99 (s, 1H). $^{13}C\{^1H\}$ NMR (125 MHz, $CDCl_3$): 8 49.1, 110.4, 119.9, 123.6, 124.3, 127.8, 130.6, 133.3, 136.6, 141.6, 141.7, 143.0, 191.5 ppm. The obtained ^{1}H NMR spectrum matches that reported previously. [44]

4-((1H benzo[d]imidazolyl-1-yl)methylbenzyl) triphenylphosphonium chloride (6)

Alcohol **3** (0.68 g, 2.84 mmol) was treated in neat $SOCl_2$ (8 cm^3, 0.1102 mol) under reflux for 30 min. The reaction progress was monitored by GC-MS. After completion, the reaction mixture was cooled to room temperature and the excess of $SOCl_2$ was removed under a vacuum to obtain a highly viscous oil. The saturated solution of Na_2CO_3 was added until the pH turned basic. Subsequently, the mixture was extracted with AcOEt (3x100 cm^3) and the collected organic portions were dried over anhydrous Na_2SO_4. The solvent was removed under a vacuum to obtain intermediate **5** as a pale yellow viscous oil that was used in further step without any purification. Chloride **5** (0.68 g, 2.64 mmol) was dissolved

in $CHCl_3$ (20 cm^3) and PPh_3 (1.04 g, 3.97 mmol) was added, and the reaction mixture was stirred at 60°C for 72 h. Dry Et_2O (30 cm^3) was added to precipitate a phosphonium salt **6** that was isolated by centrifugation. The crude material was washed with dry Et_2O (3x40 cm^3) and dried under vacuum (30°C, 15torr) to obtain a fine colourless powder (1.20 g, 88%). M.p.: 280-283 °C. Anal. Calcd. for $C_{33}H_{28}ClN_2P$ (519.02) C 76.37, H 5.44, N 5.40. Found C 76.29, H 5.58, N 5.26. ^{1}H NMR (300 MHz, DMSO-d_6): δ 5.11 (d, $^2J_{HP}$ = 15.6 Hz, 2H), 5.46 (um, 2H), 6.93 (dd, $^3J_{HH}$ = 8.2 Hz, J_{HH} = 2.4 Hz, 2H), 7.17 (d, $^3J_{HH}$ = 7.9 Hz, 2H), 7.23 (m, 2H), 7.58-7.69 (m, 15H), 7.87 (m, 2H), 8.45 (s, 1H) ppm. IR (KBr disc): 428 (w), 482 (s), 555 (m), 636 (w), 690 (s), 719 (s), 746 (s), 850 (w), 995 (w),1111 (s), 1190 (w), 1261 (w), 1284 (w), 1325 (w), 1363 (w), 1383 (w), 1437 (s), 1491 (m),1514 (w), 1612 (w), 2785 (w), 2856 (w), 2987 (w), 3055 (w), 3423 (bs) cm^{-1}. ESI-MS (pos.) m/z (%): 483.2 [M^+1^+ (100).

(E/Z)-(4,4'-Bis((1H-benzo[d]imidazol-1-yl)methyl)stilbene (7)

Compound **6** (0.90 g, 3.81 mmol) and compound **4** (1.98 g, 3.82 mmol) were dissolved in 25 cm^3 of CH_2Cl_2. Subsequently, 25 cm^3 of 0.1 M NaOH solution was added to the reaction mixture and stirred for 6 h at room temperature under a nitrogen atmosphere. The completion of the reaction was confirmed by TLC. The reaction was quenched by the addition of H_2O (50 cm^3), and the product was extracted with $CHCl_3$ (3x100 cm^3). The collected organic portions were dried over anhydrous Na_2SO_4 and evaporated using a rotary evaporator. The crude material was purified by a silica gel column eluted with a MeOH:$CHCl_3$ (2:98, v:v) system as a mixture of (E) and (Z) isomers. The ^{1}H NMR spectrum confirmed the 1:2 mixture of the (E) and (Z) isomers. The mixture appeared as a light yellow solid (1.26 g, 75% yield with respect to **6**).

^{1}H NMR of (E)/(Z) mixture (500 MHz, H_2O:DMSO-d_6, 1 :1, v:v): 5.44 (s, 4H, (Z) isomer), 5.49 (s, 4H, (E) isomer), 6.56 (s, 2H, (E) isomer), 7.117.20 (undefined multiplets, (E)/(Z) isomers), 7.29 (d, $^3J_{HH}$ = 8.3, 4H), 7.46 (um, 2H, (Z) isomer) 7.50 (um, 2H, (E) isomer), 7.53 (d, $^3J_{HH}$ = 8.3, 4H), 7.65 (um, 2H), 8.37 (s, 2H, (Z) isomer), 8.40 (s, 2H, (E) isomer) ppm. ^{1}H NMR of (E) isomer (500 MHz, DMSO-d_6): δ 5.49 (s, 4H), 7.17 (s, 2H), 7.18-7.20 (m, 4H), 7.30 (d, $^3J_{HH}$ = 8.2, 4H), 7.50 (um, 2H), 7.53 (d, $^3J_{HH}$ = 8.2, 4H), 7.65 (um, 2H), 8.40 (s, 2H) ppm. ESI-MS (pos.) m/z (%): 221.1 [M + 2H $^+$]$^{2+}$ (25), 323.1 [M + H^+ - $C_7H_6N_2$]$^+$ (21), 441.2 [M + H^+]$^+$ (100).

(E)/(Z)-(3-Methyl-1-((4-(-2-(4-((3-methyl-1H-benzo[d] zol-1-io)methyl)phenyl)vinyl)phenyl)methyl)-1H-benzo[d] imidazolium diiodide (8)

The (E)/(Z) mixture **7** (0.35 g, 0.79 mmol) was dissolved in dry DMF (10 cm^3) and CH_3I (0.123 cm^3, 1.98 mmol) was added through a micropipette. The reaction mixture was heated under a nitrogen atmosphere for 24 h at 35°C, and the reaction progress was monitored by TLC. Et_2O (25 cm^3) was added to the reaction mixture to precipitate out the product, and the solid was collected via a centrifugation process. ^{1}H NMR confirmed the formation of a (E)/(Z) mixture. The crude product was treated with a MeOH:$CHCl_3$ (1:50, v:v) system to precipitate out a yellow-coloured (E) isomer (0.18 g, 31 % yield with respect to **7**). The mother liquor containing mostly the (Z) isomer along with traces of the (E) isomer was evaporated and the (Z) isomer was purified via neutral alumina column chromatography, eluted with a MeOH:$CHCl_3$ (8:92 v:v) system to obtain a pure colourless (Z) isomer (0.35 g, 61 % yield with respect to **7**).

Physical and analytical data for (Z)-8

M.p.: 142-144 °C. Anal. Calcd. for $C_{32}H_{30}I_2N_4$ (724.42) C 53.06, H 4.17, N 7.73. Found C 52.78, H 4.28, N 7.62. ^{1}H NMR (500 MHz, DMSO-d_6): δ 4.10 (s, 6H), 5.73 (s, 4H), 6.64 (s, 2H), 7.23 (d, $^3J_{HH}$ = 8.1, 4H), 7.37 (d. $^3J_{HH}$ = 8.1, 4H), 7.65 (um, 2H), 7.70 (um, 2H), 7.89 (d. $^3J_{HH}$ = 8.2, 2H), 8.04 (d. $^3J_{HH}$ = 8.2, 2H), 9.81 (s, 2H) ppm. ^{13}C{^{1}H} NMR (126 MHz, DMSO-d_6): δ 33.4, 49.4, 113.6, 113.8, 126.6, 126.6, 128.3, 128.9, 129.9, 130.7, 132.0, 133.0, 137.0, 142.9 ppm. IR (KBr disc): 426 (w), 462 (w), 600 (w), 669 (m), 694 (w), 764 (m), 887 (w), 1016 (w), 1089 (w), 1203 (w), 1271 (w), 1296 (w), 1342(w), 1384 (w), 1457 (w), 1488 (w), 1564 (m), 1619 (m), 2341 (s), 2360 (s), 2852 (w), 2923 (w), 2962 (w), 3020 (w), 3427 (s) cmT1. ESI-MS (pos.) m/z (%): 235.0 $[M^{2+}]^{2+}$ (100) 597.1 $[M^{2+} + I^-]^+$ (10).

Physical and analytical data for (E)-8

M.p.: 270-272 °C. Anal. Calcd. for $C_{32}H_{30}I_2N_4$ (724.42) C 53.06, H 4.17, N 7.73. Found C 52.83, H 4.22, N 7.63. ^{1}H NMR (500 MHz, DMSO-d_6): δ 4.11 (s, 6H), 5.77 (s, 4H), 7.29 (s, 2H), 7.52 (d. $^3J_{HH}$ = 8.2, 4H), 7.64 (d. $^3J_{HH}$ = 8.2, 4H), 7.63-7.67 (um, 2H), 7.68-7.71 (um, 2H), 7.95 (d. $^3J_{HH}$ = 8.2, 2H), 8.04 (d. $^3J_{HH}$ = 8.2, 2H), 9.82 (s, 2H) ppm. ^{13}C{^{1}H} NMR (126 MHz, DMSO-d_6): δ 33.4, 49.6, 113.6, 113.7, 126.5, 126.6, 127.0 128.5, 128.7, 130.7, 132.0, 133.3, 137.3, 142.9 ppm. IR (KBr disc): 422 (w), 526 (w), 569 (w), 603 (w), 659 (m), 752 (s), 787 (m), 839 (w), 860 (w), 958 (w), 979 (m), 1016 (w), 1091 (w), 1128 (w), 1162 (w), 1190 (w), 1215 (m), 1278 (w), 1342 (m), 1365 (w), 1421 (w), 1448 (m), 1459 (w), 1490 (w), 1517 (w), 1564 (s), 1610 (w), 3043 (m), 3060 (w), 3129 (w), 3396 (bs), 3496 (bs) cm^{-1}. ESI-MS (pos.) m/z (%): 235.0 $[M^{2+}]^{2+}$ (100).

(E)/(Z)-3-Adamantylethyl-1-((4-(-2-(4-((3-methyl-1H benzo[d] imidazol-1-io)methyl)phenyl)vinyl)phenyl)ethyl)-1H-benzo[d] imidazolium dibromide (9)

The (E)/(Z) mixture 7 (0.05 g, 0.11 mmol) was dissolved in dry DMF (5 cm^3) and 1-(1-adamantyl)-2-bromoethane (0.08 g, 0.34 mmol) was added at once. The reaction mixture was heated under a nitrogen atmosphere for 144 h at 120 °C. The reaction progress was monitored by TLC and ESI-MS, but the reaction was never completed. A small amount of mono quaternarised intermediate was still present. Et_2O (25 cm^3) was added to the reaction mixture to precipitate out the product, and the solid was collected via a centrifugation process. The crude material was purified by silica gel chromatography eluted with a MeOH:$CHCl_3$ (10:90, v:v) system to obtain a cream-coloured **9** (0.06 g, 52% yield with respect to **7**). The ’H NMR confirmed the formation of a (E)/(Z) mixture. ^{1}H NMR (500 MHz, DMSO-d_6): δ 1.61 (s, 24H, (E)/(Z) isomers), 1.64 (d, $^2J_{HH}$ = 12.2, 12H, (E)/(Z) isomers), 1.71 (d, $^2J_{HH}$ = 12.2, 12H, (E)/(Z) isomers), 1.76 (m, 8H, (E)/(Z) isomers), 1.97 (s, 12H, (E)/(Z) isomers), 4.51 (m, 8H, (E)/(Z) isomers), 5.73 (s, 4H, (Z) isomer), 5.76 (s, 4H, (E) isomer), 6.64 (s, 2H, (Z) isomer), 7.23 (d, 3JHH = 7.9, 4H, (Z) isomer), 7.28 (s, 2H, (E) isomer), 7.39 (d, $^3J_{HH}$ = 7.9, 4H, (Z) isomer), 7.53 (d, $^3J_{HH}$ = 8.2, 4H, (E) isomer), 7.63 (d, $^3J_{HH}$ = 8.2, 4H, (E) isomer), 7.63-7.70 (m, 12H, (£)/ (Z) isomers), 7.90 (d, $^3J_{HH}$ = 8.2, 2H, (Z) isomer), 7.96 (d, $^3J_{HH}$ = 8.0, 2H, (E) isomer), 8.07 (d, $^3J_{HH}$ = 8.2, 2H, (Z) isomer), 10.02 (s, 2H, (E) isomer), 10.04 (s, 2H, (Z) isomer) ppm. ESI-MS (pos.) m/z (%): 383.2 $[M^{2+}]^{2+}$ (100).

Data for (E)-9 isomer:

M.p.: > 320 °C. Anal. Calcd. for $C_{54}H_{62}Br_2N_4 \cdot 1.7H_2O$ (957.54) C 67.73, H 6.88, N 5.85. Found C 67.72, H 6.77, N 5.98. ^{1}H NMR (300 MHz, DMSO-d_6): δ 1.61 (s, 12H), 1.65 (d, $^2J_{HH}$ = 12.2, 6H), 1.72 (d, $^2J_{HH}$ = 12.2, 6H), 1.76 (um, 4H), 1.98 (s, 6H), 4.51 (um, 4H), 5.75 (s, 4H), 7.27 (s, 2H), 7.52 (d, $^3J_{HH}$ = 7.7, 4H), 7.63 (d, $^3J_{HH}$ = 7.7, 4H), 7.65-7.67 (m, 4H), 7.96 (d, $^3J_{HH}$ = 8.0, 2H), 8.07 (d, $^3J_{HH}$ = 8.0, 2H), 9.98 (s, 2H) ppm. ^{13}C{^{1}H}

NMR (75 MHz, DMSO-d_6): δ 27.9, 31.8, 36.4., 41.4, 42.1, 42.5, 49.7, 113.9, 113.9, 126.6, 126.7, 127.0, 128.5, 128.8, 130.9, 131.2, 133.3, 137.3, 142.3 ppm. IR (KBr disc): 424 (w), 566 (w), 588 (w), 683 (w), 760 (m), 840 (w), 860 (w), 957 (w), 963 (w), 1021 (w), 1179 (w), 1196 (w), 1219 (w), 1257 (w), 1346 (w), 1370 (w), 1384 (w), 1423 (w), 1450 (m), 1479 (w), 1488 (w), 1518 (w), 1558 (m), 1609 (w), 2657 (w), 2674 (w), 2847 (m), 2900 (s), 3033 (w), 3054 (w), 3425 (bs) cm^{-1}.

REFERENCES

[1] a) D. Colin, A. Lancon, D. Delmas, G. Lizard, J. Abrossinow, E. Kahn, B. Jannin, N. Latruffe, Biochimie 2008, 90, 1674-1684; b) N. Richard, D. [32] Porath, A. Radspieler, J. Schwager, Mol. Nutr. Food Res. 2005, 49, 431442.

[2] S. J. Barrow, S. Kasera, M. J. Rowland, J. del Barrio, O. A. Scherman, [33] Chem. Rev. 2015, 115, 12320-12406.

[3] K. I. Assaf, W. M. Nau, Chem. Soc. Rev. 2015, 44, 394-418.

[4] H. Yamaguchi, Y. Kobayashi, R. Kobayashi, Y. Takashima, A. Hashidzume, A. Harada, Nat. Commun. 2012, 3, 1617/1-1617/5.

[5] A. M. Rosales, C. B. Rodell, M. H. Chen, M. G. Morrow, K. S. Anseth, J. A. Burdick, Bioconjugate Chem. 2018, 29, 905-913.

[6] Y. Wang, J.-F. Xu, Y.-Z. Chen, L.-Y. Niu, L.-Z. Wu, C.-H. Tunga, Q.-Z. Yang, Chem. Commun. 2014,50, 7001-7003.

[7] E. Z. Chernikova, D. V. Berdnikova, A. S. Peregudov, O. A. Fedorova, Z. V. Fedorov, ChemPhysChem 2019, 21, 442-449.

[8] W. Herrmann, S. Wehrle, G. Wenz, Chem. Commun. 1997, 1709-1710.

[9] S. Choi, S. H. Park, A. Y. Ziganshina, Y. H. Ko, J. W. Lee, K. Kim, Chem. Commun. 2003, 2176-2177.

[10] M. Lohse, K. Nowosinski, N. L. Traulsen, A. J. Achazi, L. K. S. von Krbek, B. Paulus, C. A. Schalley, S. Hecht, Chem. Commun. 2015, 51, 9777-9780.

[11] A. Parthasarathy, L. S. Kaanumalle, V. Ramamurthy, Org. Lett. 2007, 9, 5059-5062.

[12] a) S. P. Gromov, A. I. Vedernikov, E. N. Ushakov, N. A. Lobova, A. A. Botsmanova, L. G. Kuz'mina, A. V. Churakov, Y. A. Strelenko, M. V. Alfimov, J. A. K. Howard, D. Johnels, U. G. Edlund, New J. Chem. 2005, 29, 881-894; b) M. V. Rusalov, V. V. Volchkov, V. L. Ivanov, M. Ya. Melnikov, I. V. Shelaev, F. E. Gostev, V. A. Nadtochenko, A. I. Vedernikov, S. P. Gromov, M.V. Alfimov, Photochem. Photobiol. Sci. 2017, 16, 1801-1811.

[13] E. R. Draper, E. G. B. Eden, T. O. McDonald, D. J. Adams, Nat. Chem. 2015, 7, 848-852.

[14] V. Kolman, M. S.A. Khan, M. Babinský, R. Marek, V. Šindelář, Org. Lett. 2011, 13,6148-6151.

[15] Y. Zhou, Y. Wu, O. Pokholenko, M. Grimsrud, Y. Sham, V. Papper, R. Marks, T. Steele, Sens. Actuators B, 2018, 257, 245-255.

[16] a) D. Cameron, S. Eisler, J. Phys. Org. Chem. 2018, 31, e3858; b) E. Pazos, P. Novo, C. Peinador, A. E. Kaifer, M. D. García, Angew. Chem. Int. Ed. 2019, 58, 403-416; c) C. García-Iriepa, M. Marazzi, L.M. Frutos, D. Sampedro, RSC Adv. 2013, 3, 6241-6266.

[17] J. Szejtli, Chem. Rev. 1998, 98,1743-1753.

[18] L. Cao, M. Šekutor, P. Y. Zavalij, K. Mlinarić-Majerski, R. Glaser, L. Isaacs, Angew. Chem. Int. Ed. 2014, 53, 988-993; Angew. Chem. 2014, 126, 1006-1011.

[19] M. V. Rekharsky, Y. Inoue, Chem. Rev. 1998, 98, 1875-1918.

[20] a) M. V. Rekharsky, H. Yamamura, M. Kawai, I. Osaka, R. Arakawa, A. Sato, Y. H. Ko, N. Selvapalam, K. Kim, Y. Inoue, Org. Lett. 2006, 8, 815-818; b) P. Branná, J. Černochová, M. Rouchal, P. Kulhánek, M. Babinský, R. Marek, M. Nečas, I. Kuřitka, R. Vícha, J. Org. Chem. 2016, 81, 9595-9604; c) Y. Liu, X.-Y. Li, H.Y. Zhang, C.-J. Li, F. Ding, J. Org. Chem. 2007, 72, 3640-3645.

[21] B. Wang, J. Han, M. Bender, S. Hahn, K. Seehafer, U. H. F. Bunz, ACS Sens. 2018, 3, 504-511.

[22] Z. Yan, Q. Huang, W. Liang, X. Yu, D. Zhou, W. Wu, J. J. Chruma, C. Yang, Org. Lett. 2017, 19, 898-901.

[23] K. Jelínková, J. Kovačev^, E. Wrzecionková, Z. Prucková, M. Rouchal, L. Dastychová, R. Vícha, NewJ. Chem. 2020, 44, 7071-7079.

[24] M. W. Hanna, A. L. Ashbaugh, J. Phys. Chem. 1964, 68, 811-816.

[25] M. Rouchal, A. Matelová, F. Pires de Carvalho, R. Bernat, D. Grbić, I. Kuřitka, M. Babinský, R. Marek, R. Čmelík, R. Vícha, Supramol. Chem. 2013, 25, 349-361.

[26] P. Branná, M. Rouchal, Z. Prucková, L. Dastychová, R. Lenobel, T. Pospíšil, K. Maláč, R. Vícha, Chem. Eur. J. 2015, 21,11712-11718.

[27] P. Thordarson, Chem. Soc. Rev. 2011, 40,1305-1323.

[28] a) Rigaku, CrystalClear-SM Expert. Rigaku Americans Corporation, The Woodlands, Texas, USA, 2011; b) O.D. Rigaku, CrysAlis PRO. Rigaku Oxford Diffraction Ltd, Yarnton, Oxfordshire, England, 2015..

[29] a) G. M. Sheldrick, Acta Crystallogr. 2015, A71, 3; b) G. M. Sheldrick, Acta Crystallogr. 2015, C71, 3.

[30] D. A. Case, V. Babin, J. T. Berryman, R. M. Betz, Q. Cai, D. S. Cerutti, T. E. Cheatham III, T.A. Darden, R. E. Duke, H. Gohlke, A. W. Goetz, S. Gusarov, N. Homeyer, P. Janowski, J. Kaus, I. Kolossváry, A. Kovalenko, T. S. Lee, S. LeGrand, T. Luchko, R. Luo, B. Madej, K. M. Merz, F. Paesani, D. R. Roe, A. Roitberg, C. Sagui, R. Salomon-Ferrer, G. Seabra, C. L. Simmerling, W. Smith, J. Swails, R. C. Walker, J. Wang, R. M. Wolf, X. Wu, P. A. Kollman AMBER 16; University of California: San Francisco, 2016.

[31] R. Salomon-Ferrer, A. W. Gotz, D. Poole, S. LeGrand, R.C. Walker, J. Chem. Theory Comput. 2013, 9, 3878-3888.

[32] P. Kulhánek, T. Bouchal, I. Durník, J. Štěpán, M. Fuxreiter, L. Mones, M. Petřek, Z. Střelcová, A Toolkit for Free Energy Calculations; https:// pmflib.ncbr.muni.cz, 2018.

[33] K. N. Kirschner, A. B. Yongye, S. M. Tschampel, J. González-Outeirino, C. R. Daniels, B. L. Foley, R. J. Woods, J. Comput. Chem. 2008, 29, 622655.

[34] J.M. Wang, R.M. Wolf, J.W. Caldwell, P.A. Kollman, D. A. Case, J. Comput. Chem. 2004, 25, 1157-1174.

[35] W. Jorgensen, J. Chandrasekhar, J. Madura, R. Impey, M. Klein, J. Chem. Phys. 1983, 79,926-936.

[36] I. S. Joung, T. E. Cheatham, J. Phys. Chem. B 2008, 112, 9020-9041.

[37] J. Comer, J.C. Gumbart, J. Hénin, T. Lelievre, A. Pohorille, C. Chipot, J. Phys. Chem. B 2015, 119,1129-1151.

[38] E. Darve, D. Rodríguez-Gómez, A. Pohorille, J. Chem. Phys. 2008, 128, 144120.

[39] P. Raiteri, A. Laio, F. Gervasio, C. Micheletti, M. Parrinello, J. Phys. Chem. B 2006, 110,3533-3539.

[40] K. Minoukadeh, C. Chipot, T. Lelievre, J. Chem. Theory Comput. 2010, 6, 1008-1017.

[41] T. Stecher, N. Bernstein, G. Csányi, J. Chem. Theory Comput. 2014, 10, 4079-4097.

[42] L. Mones, N. Bernstein, G. Csányi, J. Chem. Theory Comput. 2016, 12, 5100-5110.

[43] V. Osyanin, P. Purygin, Z. Belousova, Russ. J. Gen. Chem. 2005, 75, 111117.

[44] J. J. Petraitis, Du Pont Merck Pharmaceutical Company, Wilmington Del. Preparation of (benzazolylmethyl)phenylacetaldehydes as skin antiinflammatories. USA. US 5217983A Patent.